HHS Public Access

Author manuscript

Mol Cell Neurosci. Author manuscript; available in PMC 2017 March 01.

Published in final edited form as:

Mol Cell Neurosci. 2008 July ; 38(3): 417–430. doi:10.1016/j.mcn.2008.04.003.

BMP signaling through BMPRIA in astrocytes is essential for proper cerebral angiogenesis and formation of the blood-brain-barrier

Runa Araya[1], **Moeko Kudo**[1], **Masako Kawano**[2], **Katsuyoshi Ishii**[3], **Tsutomu Hashikawa**[3], **Takuji Iwasato**[4], **Shigeyoshi Itohara**[4], **Tetsuya Terasaki**[5], **Atsuhiko Oohira**[6], **Yuji Mishina**[7,*], and **Masahisa Yamada**[1,*]

[1]Yamada Research Unit, RIKEN Brain Science Institute, Saitama, 351-0198, Japan

[2]Lab. for Cell Culture Development, RIKEN Brain Science Institute, Saitama, 351-0198, Japan

[3]Lab. for Neural Architecture, RIKEN Brain Science Institute, Saitama, 351-0198, Japan

[4]Lab. for Behavioral Genetics, RIKEN Brain Science Institute, Saitama, 351-0198, Japan

[5]Dep. of Molecular Biopharmacy and Genetics, Tohoku Univ., Sendai, 980-8578, Japan

[6]Dep. of Perinatology, Institute for Developmental Research, Aichi Human Service Center, Kasugai, Aichi 480-0392, Japan

[7]Lab. of Reproductive and Developmental Toxicology, NIEHS, Research Triangle Park, NC 27709, USA.

Abstract

Bone morphogenetic protein (BMP) signaling is involved in differentiation of neural precursor cells into astrocytes, but its contribution to angiogenesis is not well characterized. This study examines the role of BMP signaling through BMP type IA receptor (BMPRIA) in early neural development using a conditional knockout mouse model, in which *Bmpr1a* is selectively disrupted in telencephalic neural stem cells. The conditional mutant mice show a significant increase in the number of cerebral blood vessels and the level of vascular endothelial growth factor (VEGF) is significantly upregulated in the mutant astrocytes. The mutant mice also show leakage of immunoglobulin around cerebral microvessels in neonatal mice, suggesting a defect in formation of the blood-brain-barrier. In addition, astrocytic endfeet fail to encircle cortical blood vessels in the mutant mice. These results suggest that BMPRIA signaling in astrocytes regulates the expression of VEGF for proper cerebrovascular angiogenesis and has a role on in the formation of the blood-brain-barrier.

*Correspondence should be addressed to: Dr. Masahisa Yamada, Yamada Research Unit, RIKEN Brain Science Institute, Saitama 351-0198, Japan, Tel & Fax: +81 (48) 467-7648, E-mail: masahisa@brain.riken.jp**or** Dr. Yuji Mishina, Lab. of Reproductive and Developmental Toxicology, NIEHS, Research Triangle Park, NC 27709, USA, Tel: (919) 541-1095, Fax: (919) 541-3800, E-mail: mishina@niehs.nih.gov.

Introduction

Neural stem cells (NSC) are self-renewing, multipotential progenitor cells with the capacity for generating neurons and glial cells including astrocytes and oligodendrocytes. The entire surface of central nervous system is derived from NSCs in the ventricular zone, but actively dividing NSCs generate neurons in all structures of the brain. NSCs in the subventricular zone, which is formed later in embryogenesis, generate neurons, astrocytes and oligodendrocytes (Parnavelas and Nadarajah, 2001; Rao, 1999; Okano, 2002; Lennington et al 2003). Astrocytes adhere to most of the capillaries in the brain and promote formation of the blood-brain-barrier (BBB).

BMP signaling is critical for gliogenesis (Gross et al., 1996; Mabie et al, 1997; Nakashima et al., 1999a; Reiriz et al., 1999; Lim et al., 2000). For example, *in vitro* studies demonstrate that astrocytes proliferate actively and extensively branched processes formation in response to exogenous BMPs (Gross et al., 1996; Reiriz et al., 1999; D'Alessandro and Wang, 1994; Jordan et al., 1997; Angley et al., 2003). In addition, overexpression of BMP4 increases the density of astrocytes in multiple brain regions *in vivo* (Gomes et al., 2003). Several BMP ligands and receptors are expressed in the brain in a cell type-specific and developmental stage-specific manner (Zhang et al., 1998; Mekki-Dauriac et al., 2002), with higher expression during neural development and lower expression in the adult brain. BMPRIA, a type I receptor, is activated primarily by BMP2 and BMP4 (Mishina, 2003), which are expressed in the telencephalic midline (Hebert et al., 2003). BMPRIA stimulates phosphorylation and activation of Smad1, Smad5 and Smad8. Activated Smads form heteromeric complexes and bind directly or indirectly to the promoters of their respective target genes and activate target gene transcription (Derynck et al, 1998). Since disruption of *Bmpr1a* in mice blocks mesoderm formation and results in intrauterine death before embryonic day 7.5 (E7.5) (Mishina et al., 1995), a conditional allele has been generated to explore its function in neural development (Mishina et al., 2002, Mishina 2003). These attempts revealed that BMPRIA signaling is critical for dorso-ventral patterning of a developing neural tube (Wine-Lee et al., 2004) and formation of choroid plexus, the most dorsal structure of the neural tube (Hebert et al, 2002). Furthermore, it is recently shown that BMP signaling through BMPRIA is important for cell fate determination in NSCs towards glial lineage (Samanta et al., 2007), and for astrocytic maturation (See et al, 2007). Activation of BMPs signaling is thought to play a role in regulating proliferation, differentiation, and survival on vascular cells (Bobik, 2006 review), but its involvement in regulating endothelial-astrocyte interactions is not yet understood.

Angiogenesis is a multistep process that involves proliferation and migration of endothelial cells (ECs) and generation of extracellular matrix. Angiogenesis is regulated by multiple positive- and negative-regulatory factors, including vascular endothelial growth factor (VEGF), angiopoitins, interferons (alpha/beta/gamma), IL-12, tissue inhibitory metalloproteinase (TIMP)-3 and transforming growth factor-beta 1 (Campbell et al., 1999; Rivieccio et al., 2005; Zeinstra et al., 2006; Constantinescu et al., 2005; Muir et al., 2002; Dhandapani, 2005; Carmeliet, 2000; Petersen et al, 2005; Sidky and Borden, 1987; Raza and Cornelius, 2000; Dhandapani et al., 2005, 2007). VEGF, a prototypical angiogenic growth factor, regulates cell proliferation, vascular permeability, chemotaxis, and survival of ECs

and vasculogenesis and angiogenesis in the developing embryo (Ferrara et al., 2003). Astrocytes, whose endfeet encircle neural capillaries, produce angiogenesis modulating factors (Abbot, 2002; Abott et al, 2006; Lee et al., 2003), and together with ECs, play a key role in forming and maintaining the blood-brain-barrier (BBB). It has been suggested that closure of BBB is correlated to the maturation of astrocytes (DeBault and Cancilla, 1980; Janzer and Raff, 1987). VEGF and BMPs also modulate functions of peripheral ECs (Hoeben et al., 2004; Holmes and Zachary, 2005; Valdimarsdottir et al, 2002; Itoh et al., 2004).

In this study, we conditionally disrupted *Bmpr1a* in a neural stem cell-specific manner to examine the functional roles of *Bmpr1a* during neural development (Mishina, 2002, Yuhki, 2004). Our data demonstrated that BMPRIA was essential in astrocytes for down-regulation of VEGF expression during cerebral vascular angiogenesis. It was also demonstrated that BMPRIA in astrocytes played a critical role for interactions between ECs and astrocytes to form a functional BBB.

Results

BMPRIA signaling is dispensable for forming the cortical layer

Emx1$^{Cre/+}$ mice (Iwasato et al., 2000) were crossed to *CAG-CAT-LacZ* reporter mice to obtain double heterozygous (*Emx1-Cre/LacZ*) mice; these animals were used to confirm the tissue- and stage-specificity of expression of the *Emx1-Cre* transgene. At postnatal day 14 (P14), *Emx1-Cre/LacZ* mice expressed Cre recombinase [as evidenced by the staining for β-galactosidase (β-Gal) activity] in the dorsal telencephalon and in > 90% of astrocytes in the marginal zone (MZ) (Fig. 1B). Cre recombinase was also expressed in astrocytes in the upper cortical layers (Fig. 1B,D). Astrocytes along the fissura longitudinalis cerebri, the dorsal part of the telencephalon, were also positive for β-Gal (>90 %) (Fig. 1F). However, Cre recombinase was not active in astrocytes in the hypothalamic region around the third ventricle (data not shown). The immunochemical staining patterns for S100-β, a marker for astrocytes, and the staining for β-Gal activity were similar (Fig. 1, G–J). Cre recombinase was also expressed in oligodendrocytes that cross-reacted with antibody to Myelin-associated glycoprotein (MAG), 2', 3'-cyclic nucleotide 3'-phosphodiesterase (CNPase), and myelin basic protein (MBP) (Fig. 1C, Supplemental Fig.1). These results indicate that Cre-mediated recombination occurs in the majority of astrocytes in the MZ, the dorsal parts of telencephalon, the cingulate and retrosplenial cortices (Cg/RS) along the fissura longitudinalis cerebri. These results are consistent with the fact that telencephalic excitatory neurons and glial cells are believed to be derived from telencephalic neural stem cells expressing *Emx1* (Gorski et al., 2002). Lastly, we confirmed that Cre recombinase was expressed in the cortical neurons marked by Hu-protein in nucleus (Fig. 1K), but not expressed in inhibitory neurons marked by the expression of parvalbumin in the layer II, III, IV, and V (Fig. 1L). These results are in good agreement with pervious analysis for *Emx1-Cre* activity (Iwasato et al., 2000; Gorski et al., 2002).

To examine whether Cre-recombinase is expressed in non-neural cells, expression of *Emx1-Cre* was also examined in *CAG-CAT-Z* and *CMV-Z/AP* reporter gene mice. With the *CMV-Z/AP* reporter, expression of *Emx1-Cre* was confirmed in the dorsal telencephalon by

staining for alkaline phosphatase (AP) activity (data not shown). Cre recombinase-negative cells showed β-Gal activity in *Emx1-Cre/CMV-Z/AP* mice, and β-Gal activity was detected in cortical microvessels in *Emx1-Cre/CMV-Z/AP* mice (Fig. 1M). *E*xpression of Cre was examined in ECs in *Emx1-Cre/LacZ*. Expression of eNOS (Green) at P14 was examined in ECs in a middle cerebral artery of double heterozygous mice (Fig. 1N). The same section was stained with a β-Gal antibody (Red) to detect Cre activity (Fig. 1O). No β-Gal activity was detected in the area that is positive for eNOS. These results indicate that ECs were negative for *Emx1-Cre* activity.

Emx1-Cre mice were crossed with floxed-*Bmpr1a* mice. Progeny of this cross are functionally null for *Bmpr1a* in telencephalic neural stem cells, due to a Cre recombinase-mediated deletion of *Bmpr1a* exon 2 (Iwasato et al., 2000; Mishina et al., 2002). Transheterozygous mice carrying floxed-*Bmpr1a*, *Bmpr1a* null, and *Emx1-Cre* (*Emx1*$^{Cre/+}$ *Bmpr1a*$^{flox/-}$; mutant mice hereafter) were viable for more than 1 year (Yuhki et al., 2004). *In situ* hybridization showed that *Bmpr1a* was expressed in embryonic cortical cells in the ventricular zone and in differentiated neurons in *Emx1*$^{+/+}$ *Bmpr1a*$^{+/-}$ mice (control mice hereafter) at E11.5. The exon 2-specific probe failed to detect *Bmpr1a* in the mutant mice (Fig. 2A). This finding suggests that Cre-mediated recombination was complete by E11.5. The structure of cortical neural layers was normal in the mutant mice at P14 (Fig. 2A). At P20, comparable numbers of glial cells were found in the mutant mice, as evidenced by the expression of astrocytic marker GFAP or oligodendrocyte marker O4 (Fig. 2A). The mutant mice and control mice had similar numbers of TUNEL-positive neurons (data not shown).

Furthermore, tangential migration of Cajal-Retzius cells was apparently normal in the mutant mice (Fig. 2B) and the midline region and choroid plexus was present in the mutant mice (Fig. 2C–E). The morphology of cortical excitatory neurons in layer V, including the dendrites and dendritic spines of pyramidal neurons, as well as the structure of the cortical layers and the density of Hu-positive neurons were similar in the mutant and control mice (Fig. 2F). These data suggest that differentiation and migration of neural components proceeded without overt defects in the mutant mice.

Glial BMPRIA signaling is essential for the termination of angiogenesis

At E17 and P0, the number of cerebral blood vessels was comparable in the mutant and control mice (Fig. 3A,C, red arrows indicate vessels). However, the mutant mice analyzed at P10 had more cerebral blood vessels than littermate controls (Fig. 3B,C). In cortical layers II and III of the mutant mice at P10, more small blood vessels were visualized by Lectin BS-1, endothelial PECAM-1/CD31, and astroglial glutamate transporter-1 (GLT1) immunoreactivity (Fig. 3D). It is reported that expressions of PECAM-1 and GLT1 start in cerebral microvessels prior to structural maturity of the BBB (Lossinsky and Wisniewski, 1998; Matsugami et al., 2006). This analysis showed that cerebrovascular angiogenesis is altered in the mutant mice.

The phenotype of the mutant mice could be a direct consequence of the loss of *Bmpr1a* in astrocytes. However, it is also possible that loss of *Bmpr1a* in neural cells may be involved in developing the phenotypes in the mutant mice (Fig. 1). To discriminate between these two possibilities, a series of *in vitro* studies were carried out using primary astrocyte cultures

with or without targeted siRNA knockdown of *Bmpr1a*. The effect of *Bmpr1a*-targeted siRNA on gene expression was analyzed using GeneChip microarray technology (Murine Genome Array U74Av2) and RT-PCR (Fig. 4A,B). Interestingly, GeneChip analysis revealed that *Bmpr1a*-knockdown astrocytes expressed 58% more VEGF mRNA than control astrocytes (Fig. 4A), and this result was confirmed by TaqMan RT-PCR (Fig. 4B). Furthermore, Western blotting analysis revealed that *Bmpr1a*-knockdown astrocytes expressed 1.89 fold more VEGF protein than control astrocytes (Fig. 4D). It was also confirmed that expression levels of other BMP type I receptors *Bmpr1b* and *Acvr1* were comparable in *Bmpr1a*-knockdown astrocytes (data not shown). Altered levels of VEGF were also observed in the conditional mutant mice for *Bmpr1a*. In particular, GFAP-positive astrocytes in the vicinity of cerebral blood vessels were producing VEGF in the mutant mice at P10 (Fig. 4E, bottom), whereas GFAP-positive astrocytes in the control mice were either negative or in low levels of VEGF expression at P10 (Fig. 4E, top).

Production of VEGF in glial cells is essential for angiogenesis in the cortex during mouse embryonic development, and then its production is down regulated after birth (Campbell et al., 1999; Lee et al., 2003). However, high levels of VEGF were detected in the neonatal mutant mice, suggesting that angiogenesis might continue in the mutants after birth. These results suggest that BMPRIA signaling downregulates VEGF in astrocytes during cerebrovascular angiogenesis. GeneChip analyses showed that expression levels of inhibitors of angiogenesis were not changed between the mutant and control mice, such as Endostatin, Interferon alpha/beta/gamma, Interleukin-12a/b, Plasminogen activator inhibitor, Platelet factor-4, Prolactin, Proliferin-related protein, TIMP-3, and TGF-beta 1. Thus, it is likely that the increased expression of VEGF in astrocytes in the vicinity of cerebral microvessels directly stimulates angiogenesis in the mutant mice.

Glial BMPRIA plays a critical role in formation of the BBB

During postnatal development, astrocyte endfeet encircle the endothelial layers of capillary blood vessels. ECs, which are activated by angiogenic factors, produce basement membrane that facilitates their migration. Adhesion molecules or integrins promote interactions between ECs and astrocyte endfeet, and sprouting ECs roll up to form functional blood vessels (McCarty et al., 2002). By P19, angiogenesis is mostly complete and tight junctions have formed in cerebral microvessels. The aforementioned steps lead to the establishment of a functional BBB by P19 (Lee et al., 2003). Because BMPs stimulate interactions between cell adhesion molecules and astrocytes (D'Alessandro et al., 1994), the structure of cerebral microvessels was examined in the mutant and control mice after birth (*i.e.*, P10 and P20). Cerebral vasculature microstructure was examined from MZ to layer VI and in the Cg/RS by electron microscopy. At E17, the endfeet of astrocytes were already associated with ECs in the control or mutant mice with a space separated vessels from the underlying brain parenchymal cells (Fig. 5A,B, black arrow). At P10, astrocytic endfeet started to encircle the vessels in the control (Fig. 5C. red arrow indicates endfeet), but in the mutant mice, blood vessels with a rarefied area around the vessels were observed instead of the endfeet membrane-component (Fig. 5D, black arrow). Furthermore, cerebral blood vessels that were composed with multiple-ECs and enlarged vessels were observed in layers II / III of the mutant mice (Fig. 5E and 5F, respectively). These results indicate that cerebral blood vessels

in the mutant mice were structurally abnormal as early as P10, before the BBB becomes stable. In control mice cortex, arterioles penetrate the cortical layers I and II / III from the surface and give rise to capillaries to produce a pattern of radially penetrating vessels. However, sequential observation of the section shown in Fig. 3D and its adjacent sections revealed that the orientation of arterioles appeared randomly in the mutant mice (data not shown). From the morphological characteristics, we classified structure of blood vessels in four types: encirclement-type, rarefied area-type, enlargement-type, and multiple ECs-type at P10 (Fig. 5D–F). Those rarefied area-type and multiple ECs-type were not seen in normal control sections. The mutant mice showed decrease in the ratio of encirclement-type, and increase in the ratio of enlargement-type, rarefied area-type and multiple ECs-type (FIG. 5K).

Astrocytes in P20 control mice made contact with and formed astroglial endfeet around cerebral blood vessels in the superficial cortex and in the Cg/RS (Fig. 5G, red arrow indicates endfeet). However, astrocytes in the mutant mice did not form similar structures around the basal lamina of the capillary ECs in layers II / III at P20 (Fig. 5H–J, black arrow; red arrow indicates endfeet).

The function of the BBB was examined by injecting 25 mg/kg Evans blue into the tail vein of the control and mutant mice followed by visualization of auto-fluorescence of EB in cortical tissues (Saria and Lundberg, 1983). Since EB binds to albumin, red fluorescence observed in tissues indicate leakage of blood vessels. At P10, fluorescence of EB was detected in tissues surrounding cortical blood vessels including the dorsal telencephalon and Cg/RS along the fissura longitudinalis cerebri in the mutant mice (Fig. 6B,D). In the mutant mice at P20, there was evidence of leakage into the superficial cortex and the Cg/RS along the fissura longitudinalis cerebri (Fig. 6F,G). No leakage was detected in the corresponding areas of the control mice (Fig. 6E). It was noted that no leakage was detected in layer V of the mutant mice (data not shown), which was in good agreement with the distribution of Cre activities in astrocytes (Fig. 1B,D). These results indicate that a stable BBB has not formed in the P10 or P20 mutant mice, likely due to the failure of encirclement of astrocytic endfeet around cerebral ECs (Fig. 5J).

Leakage of immunoglobulin was also detected in the MZ of 10-month-old mutant mice, but not in the same region of control mice (Fig. 6H,I). The number of apoptotic cells (as detected by TUNEL assay and the presence of caspase-3) was higher in the superficial cortex and the Cg/RS of the mutant mice than in the control mice at P20 (Supplemental Fig. 2). However, cell death did not increase in cortical microvessels in the ventricular zone of the mutant mice (data not shown). Leakage of immunoglobulin was not detected in the ventricular amygdala region or the piriform cortex of the 10-month-old mutant mice (Fig. 6J). These data indicate that malformation of a BBB is evident in the mutant mice by P20, and leakage of blood proteins persists in the adult mice.

The failure of astrocytic endfeet to attach to ECs could be due to insufficient expression of adhesion molecules in *Bmpr1a*-deficient astrocytes in the mutant mice. This idea was tested by measuring expression of adhesion molecules and the adhesive properties of cultured primary astrocytes with or without targeted siRNA-mediated knockdown of *Bmpr1a*.

GeneChip analysis revealed reduced expression of adhesion molecules in the *Bmpr1a* knockdown cells. Downregulated genes included Type I, Type III, and Type IV pro-collagens (Fig. 7A), which are thought to be essential for endothelial cell-astrocyte interactions (Tagami et al., 1992). TaqMan real-time RT-PCR confirmed the results of the GeneChip analysis (Fig. 7B). These data support the idea that *Bmpr1a*-deficiency in astrocytes interferes with astrocyte-endothelial interactions and leads to structural instability of the BBB in the mutant mice.

Next, we examined expression levels of neurocan, a reactive astrocytic marker (Asher et al., 2000). Neurocan is normally expressed in embryonic neural stem cells, but its expression decreases rapidly after birth in wild type mice (Sango et al., 2003; Ida et al., 2006). In contrast, neurocan was expressed at P10 around cortical blood vessels in the mutant mice (data not shown) and was strongly upregulated in the MZ and the Cg and RSG cortices along the fissura longitudinalis cerebri in the mutant mice at 10 month (Fig. 8A). The fact that neurocan lowered adhesion ability of endothelial cell lines TM-BBB (Hosoya et al., 2000) (Fig. 8B) and HUVEC cells (Fig. 8C) in culture suggests that neurocan might interfere with the adhesive properties of astrocytes and/or ECs. Because expression of neurocan mRNA did not change in astrocytes treated with *Bmpr1a*-targeted siRNA (Fig 7A,B), upregulation of neurocan at P10 in mutant mice may be a secondary effect of the failure to form the BBB. As stated above, these results suggest that *Bmpr1a*-deficient astrocytes have reduced capacity for cellular adhesion, which may lead to defective formation of the BBB in the mutant mice. Furthermore, constitutive production of neurocan in astrocytes in the mutant mice may also interfere the formation of the BBB in these animals.

Discussion

Previous studies demonstrate that BMP signaling plays significant roles in patterning of the medial-lateral axis during early neural development (Furuta et al., 1997; Hebert et al., 2002) and in gliogenesis during late neural development (Gross et al., 1996; Mabie et al, 1997; Nakashima et al., 1999a; Reiriz et al., 1999; Lim et al., 2000; Gomes et al., 2003). This study provides evidences that BMP signaling through BMPRIA regulates cerebrovascular angiogenesis, modulates interactions between ECs and astrocytes, and is essential for formation of a functional BBB. Using the *Emx1*-Cre mice that express Cre recombinase in a telencephalic neural stem cell-specific manner, we show that loss of *Bmpr1a* leads to upregulation of VEGF in astrocytes and dysfunctional attachments between astrocytic endfeet and ECs. The latter observation could reflect decreased expression of adhesion molecules in *Bmpr1a*-deficient astrocytes. Taken together, our results strongly suggested that BMPRIA signaling regulates the balance between pro- and anti-angiogenic factors and modulates endothelial cell-glial interactions during neural development.

Since *Emx1*-Cre is expressed in neural stem cells, it is formally possible that the phenotype of mutant mice, at least in part, are due to the loss of BMPRIA in other types of cells than astrocytes that are also derived from neural stem cells. However, no significant morphological changes were observed in blood vessels in layer V, where Cre activity in astrocytes was much lower than that in MZ and layer II / III in the mutant mice (Fig. 1B).

Distributions of abnormal structure of astrocyte-endothelial junctions surrounding cerebral blood vessels were associated with these of *Bmpr1a*-deficient astrocytes (Cre activity) but not with those of oligodendrocytes or neurons. These results suggest that BMP signaling in astrocytes, but not in other cell types, plays a significant role in interactions between astrocytes and ECs, leading to malformation of the BBB in the mutant mice.

It is recently reported that conditional disruption of *Bmrp1a* using an *Olig1* promoter driven Cre transgenic line lead to a significant increase in the number of mature and immature oligodendrocytes as well as inhibitory neurons (Samanta et al., 2007). In the mutant mice using the *Emx1*-Cre mice described here, the number of oligodendrocytes was not dramatically changed assessed by production of O4 (Fig. 2A). *Olig1* is expressed in neural progenitors especially in the ventricular zone of medial and lateral ganglionic eminences at E12.5 (Bansal et al., 2003). On the other hand, *Emx1* is expressed in the progenitors of excitatory neurons in ventricular zone. In the present study, we found that Cre recombinase was also expressed in oligodendrocytes that cross-reacted with antibody to MAG, CNPase, and MBP (Fig. 1C, Supplemental Fig.1). These differences for expression domains of Cre recombinase may account for the different outcomes for the numbers of oligodendrocytes after removal of BMPRIA signaling.

It is also recently reported that double mutant mice for BMP type I receptors *Bmpr1a* and *Bmpr1b* exhibited a 25–40% decrease in GFAP-positive or S100β-positive astrocytes in the cervical spinal cord (See et al., 2007). This result shows an interesting contrast to ours in terms of the numbers of astrocytes. The Cre line used to generate the double mutant mice starts to express Cre recombinase much earlier stage than *Emx1*-Cre (Ahn et al., 2001). It would raise an intriguing possibility that function of BMPRIA signaling in developing neural tissues may be different if stages and/or regions are different. Detailed comparative analyses of these conditional mutant mice would provide further insights for this issue. Nonetheless, both *Olig1*-Cre induced disruption of *Bmpr1a* and the double mutation for BMP type I receptors result in perinatal lethality, and present analyses revealed as the first time that the importance of the BMPRIA signaling for cerebral vessel formation and BBB formation after birth.

Cerebrovascular angiogenesis is regulated by pro-angiogenic growth factors and angiogenesis inhibitors (the positive or negative regulation for angiogenesis). VEGF, a potent angiogenic factor, is present in developing blood vessels during embryonic neurogenesis, but is not detected in the mature vasculature. Retinal astrocytes also express VEGF, which promotes endothelial cell proliferation and migration (Alon et al., 1995; Stone et al., 1995; Pierce et al., 1996; Provis et al., 1997), however, developing blood vessels trigger astrocyte differentiation leading to suppression of VEGF expression (West et al., 2005). Recent studies demonstrated that vascular endothelial cells produce BMPs (Sorescu et al., 2003; Shin et al, 2004), and that BMP2 and LIF cooperatively induce astrocyte differentiation in the developing mouse brain (Nakashima et al., 1999b). We found that upregulation of VEGF production in the astrocytes of the mutant mice at P10. Together, these facts suggest that BMPs produced by vascular endothelial cells interact with BMPRIA in the astrocytes and the BMPRIA-mediated signaling downregulates VEGF production in astrocytes for normal cerebrovascular angiogenesis.

When *Bmpr1a* was knocked down by siRNA in primary cultured astrocytes, expressions of collagens, which play an important role in adhesion between astrocytes and ECs, were significantly down regulated (Sango et al., 2003; Brightman, 2002). It is reported that intracellular SMAD signaling induces expression of extracellular matrix (ECM) and basement membrane components in cultured astrocytes via Type IV pro-collagens (Fuchshofer et al., 2005; Gaussin, 2002; Jackson et al., 2003). ECM components regulated by SMAD signaling direct remodeling of blood vessels in some internal organs such as the lung or liver (Ng et al., 2005; Fernandez-L A, 2006). Thus, *Bmpr1a* plays a role in cell adhesion capacity in these tissues. Integrins are also thought to play a role in astrocyte adhesion (Fasen et al., 2003); however, the expression levels of integrin subunits α1, α2, α4, α5, α6, α3, and α4, were similar in wild type and the mutant mice (data not shown). Expression of Cadherin 1 (E-cadherin) and Cadherin 4 (R-cadherin), which also play a role in cellular adhesion (Abbruscato and Davis, 1999; Dorrell et al., 2002) were unchanged in the mutant mice (data not shown). In addition to the downregulation of aforementioned cell adhesion molecules in the mutant mice, persistent production of neurocan in the mutant mice may lead to the disruption of cell clustering, which negatively affects the formation of the proper BBB. This is an interesting possibility because regions where an inflammation is induced (Fig. 6F, I) are well overlaps with the regions where *Emx1*-Cre is expressed (Fig. 1B, D) and failure of proper BBB formation is frequently found. It is reported that neurocan produced sites of inflammation show repressive effects of adhesion against nearby neurons (Asher et al., 2000). This is an alternative, not exclusive, explanation why interactions between astrocytes and ECs are less affected in layer V, where production of neurocan is hardly detected. The relationship between BMP signals and the control of adhesion ability of astrocytes both *in vivo* and in cultured system is an interesting area for future research. Our results suggest that ECM components may belong to the members of the signaling cascade on vascular formation, although the identity of adhesive molecules that act downstream of BMP signaling are largely unknown.

In conclusion, this study demonstrates that BMP signaling through BMPRIA regulates cerebrovascular angiogenesis and modulates interactions between ECs and astrocytes. In particular, BMPRIA-signaling downregulates VEGF expression and modulates the adhesive properties of astrocytes during neural development to develop normal cerebrovascular systems.

Experimental methods

Generation of Mouse Lines

For evaluation of the Cre activities, $Emx1^{Cre/+}$ mice were bred with *CAG-CAT-Z* reporter mice (Sakai and Miyazaki, 1997), and double heterozygous (*Emx1-Cre/LacZ*) mice were obtained. We crossed $Emx1^{Cre/+}$ mice with *CMV-Z/AP* reporter mice (Lobe et al., 1999), and obtained double heterozygous (*Emx1-Cre/AP*$^{+}$) mice. *Emx1-Cre* mice and floxed-*Bmpr1a* mice were maintained as previously described (Yuhki et al., 2004). The present study was carried out according to the Guide for the Care and Use of laboratory animals in the Guidelines of the Society for Neuroscience and under an approved animal protocol from the Animal Care and Use Committee of RIKEN and NIEHS.

Histology

Immunostaining were performed as described (Yuhki et al., 2004). Cryostat sections of embedded embryos were made at −24 °C. Frozen cryosections (15 μm) were treated with 3% H_2O_2, incubated with blocking buffer (PBS containing 0.01% Triton and 1.5% normal goat serum), and incubated overnight at 4°C with primary antibodies. Immunostaining was performed as described (Yuhki et al., 2004). Sections were incubated with secondary antibody in blocking buffer for 1 h at room temperature; a DAB detection system was used (Perkin Elmer Life Sciences). The primary antibodies used were anti beta-galactosidase Ab (Cappel), anti-cleaved caspase 3 Ab (Cell Signaling Technology), anti Cre recombinase Ab (Covance Babco), anti-eNOS Ab (BD Transduction Laboratory), anti-GFAP Ab (DAKO), anti-human placental alkaline phosphatase polyclonal Ab (Biomeda), anti-human placental alkaline phosphatase Ab (SIGMA), anti-Neurocan Ab (Asher, 2000), anti-Thymosin-β4 Ab (Sapp et al., 2001), anti-O4 (a gift from Dr. Steve Pfeiffer, University of Connecticut), anti-CNPase Ab (CHEMICON), anti-MBP Ab (CHEMICON), anti-Caspase-3 Ab (Cell Signaling), ant-S100β Ab (SWant), anti-MAG (myelin-associated glycoprotein) Ab (a gift from Dr. Keiichi Uyemura, Keio University), anti-Calretinin Ab (SWant), and anti-MAP2 Ab (CHEMICON). Secondary antibodies were FITC–conjugated goat anti–mouse IgG (Jackson Immunoresearch), Cy3–conjugated goat anti–rabbit IgG (Jackson Immunoresearch), alexa fluor 546 goat anti-mouse IgG (Molecular Probes), alexa fluor 488 goat anti-rabbit IgG (Molecular Probes), goat anti-mouse IgG-peroxidase (MBL), goat anti-rabbit IgG–peroxidase (MBL), SA-Fluorescein (Perkin Elmer Life Sciences), SA-Texas red (Perkin Elmer Life Sciences), biotinylated anti-mouse IgG antibody (Vector Laboratories). Sections were counterstained with Hoechst (CALBIOCHEM). For DAB reaction of Caspase-3 staining, sections were incubated in biotinylated anti-rabbit IgG antibody (Vector Laboratories) diluted in blocking buffer.

Electron-micrograph

Brains from the control and mutant mice at postnatal day 10 or 20 were transcardially perfused with 0.9% NaCl (200 ml/kg body weight) followed by 2.5% glutaraldehyde and 2% paraformaldehyde in 0.1 M phosphate buffer (PB) for 15 minutes. The cerebral cortices were sectioned at 200 mm in the coronal section. The dorsomedial region of the parietal cortex was postfixed with 2% (w/v) osmium tetroxide in 0.1 M PB, dehydrated in a graded ethanol series, and flat-embedded in epoxy resin (Araldyte CY212, TAAB). Ultrathin sections (80 nm Ultracut-UCT, Leica) were stained with uranyl acetate and lead citrate. Electron micrographs were recorded on imaging plates through an LEO 912 electron microscope (LEO electron microscopy). Images were scanned and digitized using an FDL 5000 imaging system (Fuji Photofilm).

Cell attachment

For experiments with ECs, 48-well tissue culture plates (Nalge Nunc International) were coated with (1) Poly-L-lysine (10 μg/ml) (PL, Sigma) (control), (2) Neurocan (10 μg/ml, 1 μg/ml, 0.1 μg/ml) or (3) PL and collagen (20 μg/ml; TOYOBO) (CL). Neurocan was purified from postnatal rat brain as described previously (Oohira et al., 1991, Inatani et al., 2001). PL diluted in distilled water was applied to each well for 1 h at room temperature. PL was air-

dried for 1 h, and PL-coated plates were treated immediately with additional substrates for 1 h at room temperature. HUVEC and TM-BBB cells (Hosoya et al., 2000) were suspended in a medium (Endothelial Cell Basal Medium with Endothelial Cell growth Supplement (CELL APPLICATIONS, INC.) for HUVEC cells, or DMEM with 10% FBS and 15 μg/ml ECGF (Roche) for TM-BBB cells) and seeded on the coated wells. Cell density was adjusted to 1×10^4/ cm^2 cells and cells were allowed to adhere for 3 h. Adherent cells were washed three times to exclude non-attached cells. The numbers of viable adherent and total cells were counted under the microscope.

Mouse astrocytes primary culture

For primary mouse astrocyte culture, astrocytes were isolated from embryonic day 17 (E17) cerebral hemispheres of BL6 mice. Dissociated glial cells were prepared as described before (Yamada et al., 1999). Plated glial cells were allowed to grow for a 14 days, and processed for siRNA treatments. 48-well tissue culture plates (Nalge Nunc International) were coated with the following substrates Poly-L-lysine (10 μg/ml) (PL, Sigma). *Bmpr1a*-targeted siRNA treated astrocytes were suspended in 2.5% FBS DMEM and seeded on the coated wells. The density of cells was adjusted to 1000 per well and cells were allowed to adhere to the substratum for 2 h.

DNA chip profiling

We carried out high-density oligonucleotide array gene expression studies with extracts from siRNA-treated astrocytes. Results were compared using specific and nonspecific siRNA (GeneChip; Affymetrix). An Affymetrix algorithm (Lipshutz et al., 1999) (i.e., multiple analysis comparison software) was used to quantify gene expression changes. Significant changes were observed in expression of the following genes: *Procollagen Type I alpha 1*, U034191; *Procollagen Type III alpha 1*, X52046; *Procollagen Type IV alpha 1*, M15832; *Integrin alpha 1*, AK035870; *Integrin alpha 2*, X75427; *Integrin alpha 4*, X69902; *Integrin alpha 5*, X79003; *Integrin beta 3*, AF026509; *Integrin beta 4*, L04678; *Cadherin 1*, X60961; *Cadherin 4*, X69966 *Neurocan*, D16250; *Bmpr1a*, X84727. No changes were observed in expression of the following genes: *Endostatin, U03715; Interferon alpha, L38698; Interferon beta, K00020; Interferon gamma, K00083; Interleukin-12a, M86672; Interleukin-12b, M86671; Plasminogen activator inhibitor II, X16490; Platelet factor-4, AB017491; Prolactin, X04418; Proliferin-related protein, tissue inhibitor of metalloproteinases-3 (TIMP-3), U26437; Transforming growth factor-beta 1, AJ009862*.

TaqMan RT-PCR

The TaqMan primer and probe sets were designed with Primer Express software (Applied Biosystems). Applied Biosystems Assay IDs are noted (*Procollagen* Type I alpha 1, Mm00801666_g1; *Procollagen* Type III alpha 1, Mm00802331_m1; *Procollagen* Type IV alpha 1, Mm00802372_m1; *Neurocan*, Mm00484007_m1; *Bmpr1a*, Mm00477650_m1 ; *Bmpr1b*, Mm00432117_m1; *vegf*, Mm00437304_m1). TaqMan RT–PCR was performed using the extracts for astrocytes treated with *Bmpr1a*-targeted siRNA or control nonspecific siRNA (n = 4). All values were to glyceraldehyde-3-phosphate dehydrogenase (GAPDH).

Immunoblotting

Cell lysates were prepared in an appropriate volume of RIPA buffer (50 mM Tris-HCl, pH 7.5, 150 mM NaCl, 1% Na-Deoxycholate, 0.1% SDS, 1% Triton X-100, 0.4 mM EDTA, 1 mM EGTA) with protease inhibitors. 100 μg cell lysates were separated by SDS–PAGE, probed with the anti-VEGF polyclonal antibody (LAB VISION).

Stability of cerebral blood vessels

Mice were anesthetized with pentobarbital and Evans blue (EB, 0.5% solution in 0.9% NaCl) was injected through tail vein (25 mg/kg). After six hours, mice were anesthetized with pentobarbital and perfused with 4%-formaldehyde neutral buffer. The brains were removed and post-fixed for 6 hours. The brains were stored at −24 °C and cryostat sections were made 12 hours later. Auto-fluorescence was visualized using excitation at 620 nm and emission at 680 nm.

Supplementary Material

Refer to Web version on PubMed Central for supplementary material.

Acknowledgments

We thank Drs. J. Harry, M. Ray, H. Hama, M. Yuhki, and M. Ogawa, for their kind advice. We thank N. Kitamura, H. Kishida, and Y. Sakamaki (RIKEN BSI-RRC) for their expert technical assistance. The *CAG-CAT-LacZ* reporter mice were provided by Dr. J. Miyazaki. This work was supported by MEXT Grant-in-Aid for Young Scientists (B) and #16047231 to M.Y. and by the Intramural Research Program of the NIEHS, NIH (ES071003-10) to Y. M

References

Abbott N. Astrocyte-endothelial interactions and blood-brain barrier permeability. J Anat. 2002; 200:527.

Abbott NJ, Ronnback L, Hansson E. Astrocyte-endothelial interactions at the blood-brain barrier. Nat Rev Neurosci. 2006; 7:41–53. [PubMed: 16371949]

Abbruscato TJ, Davis TP. Protein expression of brain endothelial cell E-cadherin after hypoxia/aglycemia: influence of astrocyte contact. Brain Res. 1999; 842:277–286. [PubMed: 10526124]

Ahn K, Mishina Y, Hanks MC, Behringer RR, Crenshaw EB 3rd. BMPR-IA signaling is required for the formation of the apical ectodermal ridge and dorsal-ventral patterning of the limb. Development. 2001; 128:4449–4461. [PubMed: 11714671]

Alon T, Hemo I, Itin A, Pe'er J, Stone J, Keshet E. Vascular endothelial growth factor acts as a survival factor for newly formed retinal vessels and has implications for retinopathy of prematurity. Nat. Med. 1995; 1:1024–1028. [PubMed: 7489357]

Angley C, Kumar M, Dinsio KJ, Hall A, Siegel RE. Signaling by bone morphogenetic proteins and Smad1 modulates the postnatal differentiation of cerebellar cells. J. Neurosci. 2003; 23:260–268. [PubMed: 12514223]

Asher RA, Morgenstern DA, Fidler PS, Adcock KH, Oohira A, Braistead JE, Levine JM, Margolis RU, Rogers JH, Fawcett JW. Neurocan is upregulated in injured brain and in cytokine-treated astrocytes. J Neurosci. 2000; 20:2427–2438. [PubMed: 10729323]

Bansal R, Lakhina V, Remedios R, Tole S. Expression of FGF receptors 1, 2, 3 in the embryonic and postnatal mouse brain compared with Pdgfralpha, Olig2 and Plp/dm20: implications for oligodendrocyte development. Dev Neurosci. 2003; 25:83–95. [PubMed: 12966207]

Bobik A. Transforming growth factor-betas and vascular disorders. Arterioscler Thromb Vasc Biol. 2006; 26:1712–1720. [PubMed: 16675726]

Brightman MW. The brain's interstitial clefts and their glial walls. J Neurocytol. 2002; 31:595–603. [PubMed: 14501201]

Campbell IL, Krucker T, Steffensen S, Akwa Y, Powell HC, Lane T, Carr DJ, Gold LH, Henriksen SJ, Siggins GR. Structural and functional neuropathology in transgenic mice with CNS expression of IFN-alpha. Brain Res. 1999; 835:46–61. [PubMed: 10448195]

Carmeliet P, Ferreira V, Breier G, Pollefeyt S, Kieckens L, Gertsenstein M, Fahrig M, Vandenhoeck A, Harpal K, Eberhardt C, Declercq C, Pawling J, Moons L, Collen D, Risau W, Nagy A. Abnormal blood vessel development and lethality in embryos lacking a single VEGF allele. Nature. 1996; 380:435–439. [PubMed: 8602241]

Constantinescu CS, Tani M, Ransohoff RM, Wysocka M, Hilliard B, Fujioka T, Murphy S, Tighe PJ, Sarma JD, Trinchieri G, Rostami A. Astrocytes as antigen-presenting cells: expression of IL-12/IL-23. J Neurochem. 2005; 95:331–340. [PubMed: 16086689]

D'Alessandro JS, Wang EA. Bone morphogenetic proteins induce differentiation in astrocyte lineage cells. Growth Factors. 1994; 11:53–69. [PubMed: 7530466]

DeBault LE, Cancilla PA. gamma-Glutamyl transpeptidase in isolated brain endothelial cells: induction by glial cells in vitro. Science. 1980; 207:653–655. [PubMed: 6101511]

Derynck R, Zhang Y, Feng XH. Smads: transcriptional activators of TGF-beta responses. Cell. 1998; 95:737–740. [PubMed: 9865691]

Dhandapani KM, Wade FM, Mahesh VB, Brann DW. Astrocyte-derived transforming growth factor-{beta} mediates the neuroprotective effects of 17{beta}-estradiol: involvement of nonclassical genomic signaling pathways. Endocrinology. 2005; 146:2749–2759. [PubMed: 15746252]

Dhandapani KM, Khan MM, Wade FM, Wakade C, Mahesh VB, Brann DW. Induction of transforming growth factor-beta1 by basic fibroblast growth factor in rat C6 glioma cells and astrocytes is mediated by MEK/ERK signaling and AP-1 activation. J Neurosci Res. 2007; 85:1033–1045. [PubMed: 17335076]

Dorrell MI, Aguilar E, Friedlander M. Retinal vascular development is mediated by endothelial filopodia, a preexisting astrocytic template and specific R-cadherin adhesion. Invest Ophthalmol Vis Sci. 2002; 43:3500–3510. [PubMed: 12407162]

Fasen K, Elger CE, Lie AA. Distribution of alpha and beta integrin subunits in the adult rat hippocampus after pilocarpine-induced neuronal cell loss, axonal reorganization and reactive astrogliosis. Acta Neuropathol (Berl). 2003; 106:319–322. [PubMed: 12851778]

Ferrara N, Gerber HP, LeCouter J. The biology of VEGF and its receptors. Nat Med. 2003; 9:669–676. [PubMed: 12778165]

Fernandez-L A, Sanz-Rodriguez F, Blanco FJ, Bernabeu C, Botella LM. Hereditary hemorrhagic telangiectasia, a vascular dysplasia affecting the TGF-beta signaling pathway. Clin Med Res. 2006; 4:66–78. [PubMed: 16595794]

Fuchshofer R, Birke M, Welge-Lussen U, Kook D, Lutjen-Drecoll E. Transforming growth factor-beta 2 modulated extracellular matrix component expression in cultured human optic nerve head astrocytes. Invest Ophthalmol Vis Sci. 2005; 46(2):568–578. [PubMed: 15671284]

Furuta Y, Piston DW, Hogan BLM. Bone morphogenetic proteins (BMPs) as regulators of dorsal forebrain development. Development. 1997; 124:2203–2212. [PubMed: 9187146]

Gaussin V, Van de Putte T, Mishina Y, Hanks MC, Zwijsen A, Huylebroeck D, Behringer RR, Schneider MD. Endocardial cushion and myocardial defects after cardiac myocyte-specific conditional deletion of the bone morphogenetic protein receptor ALK3. Proc Natl Acad Sci U S A. 2002; 99:2878–2883. [PubMed: 11854453]

Gomes WA, Mehler MF, Kessler JA. Transgenic overexpression of BMP4 increases astroglial and decreases oligodendroglial lineage commitment. Dev Biol. 2003; 255:164–177. [PubMed: 12618141]

Gorski JA, Talley T, Qiu M, Puelles L, Rubenstein JL, Jones KR. Cortical excitatory neurons and glia, but not GABAergic neurons, are produced in the Emx1-expressing lineage. J. Neurosci. 2002; 22:6309–6314. [PubMed: 12151506]

Gross RE, Mehler MF, Mabie PC, Zang Z, Santschi L, Kessler JA. Bone morphogenetic proteins promote astroglial lineage commitment by mammalian subventricular zone progenitor cells. Neuron. 1996; 17:595–606. [PubMed: 8893018]

Hebert JM, Mishina Y, McConnell SK. BMP signaling is required locally to pattern the dorsal telencephalic midline. Neuron. 2002; 35:1029–1041. [PubMed: 12354394]

Hebert JM, Hayhurst M, Marks ME, Kulessa H, Hogan BL, McConnell SK. BMP ligands act redundantly to pattern the dorsal telencephalic midline. Genesis. 2003; 35:214–219. [PubMed: 12717732]

Hoeben A, Landuyt B, Highley MS, Wildiers H, Van Oosterom AT, De Bruijn EA. Vascular endothelial growth factor and angiogenesis. Pharmacol Rev. 2004; 56:549–580. [PubMed: 15602010]

Holmes DI, Zachary I. The vascular endothelial growth factor (VEGF) family: angiogenic factors in health and disease. Genome Biol. 2005; 6:209. [PubMed: 15693956]

Hosoya K, Tetsuka K, Nagase K, Tomi M, Saeki S, Ohtsuki S, Takanaga H, Yanai N, Obinata M, Kikuchi A, Okano T, Terasaki T. Conditionally immortalized brain capillary endothelial cell lines established from a transgenic mouse harboring temperature-sensitive simian virus 40 large T-antigen gene. AAPS PharmSci. 2000; 2:E27. [PubMed: 11741243]

Ida M, Shuo T, Hirano K, Tokita Y, Nakanishi K, Matsui F, Aono S, Fujita H, Fujiwara Y, Kaji T, Oohira A. Identification and functions of chondroitin sulfate in the milieu of neural stem cells. J Biol Chem. 2006; 281:5982–5991. [PubMed: 16373347]

Inatani M, Honjo M, Otori Y, Oohira A, Kido N, Tano Y, Honda Y, Tanihara H. Inhibitory effects of neurocan and phosphacan on neurite outgrowth from retinal ganglion cells in culture. Invest Ophthalmol Vis Sci. 2001; 42:1930–1938. [PubMed: 11431463]

Itoh F, Itoh S, Goumans MJ, Valdimarsdottir G, Iso T, Dotto GP, Hamamori Y, Kedes L, Kato M, ten Dijke PtP. Synergy and antagonism between Notch and BMP receptor signaling pathways in endothelial cells. EMBO J. 2004; 23:541–551. [PubMed: 14739937]

Iwasato T, Datwani A, Wolf AM, Nishiyama H, Taguchi Y, Tonegawa S, Knopfel T, Erzurumlu RS, Itohara S. Cortex-restricted disruption of NMDAR1 impairs neuronal patterns in the barrel cortex. Nature. 2000; 406:726–731. [PubMed: 10963597]

Jackson LF, Qiu TH, Sunnarborg SW, Chang A, Zhang C, Patterson C, Lee DC. Defective valvulogenesis in HB-EGF and TACE-null mice is associated with aberrant BMP signaling. EMBO J. 2003; 22:2704–2716. [PubMed: 12773386]

Janzer RC, Raff MC. Astrocytes induce blood-brain barrier properties in endothelial cells. Nature. 1987; 325:253–257. [PubMed: 3543687]

Jordan J, Bottner M, Schluesener HJ, Unsicker K, Krieglstein K. Bone morphogenetic proteins: neurotrophic roles for midbrain dopaminergic neurons and implications of astroglial cells. Eur J Neurosci. 1997; 9:1699–1709. [PubMed: 9283824]

Lee SW, Kim WJ, Choi YK, Song HS, Son MJ, Gelman IH, Kim YJ, Kim KW. SSeCKS regulates angiogenesis and tight junction formation in blood-brain barrier. Nat Med. 2003; 9:900–906. [PubMed: 12808449]

Lennington JB, Yang Z, Conover JC. Neural stem cells and the regulation of adult neurogenesis. Reprod Biol Endocrinol. 2003; 1:99. [PubMed: 14614786]

Lim DA, Tramonti AD, Trevejo JM, Herrera DG, Garcia-Verdugo JM, Alvarez-Buylla A. Noggin antagonizes BMP signaling to create a niche for adult neurogenesis. Neuron. 2000; 28:713–726. [PubMed: 11163261]

Lipshutz RJ, Fodor SP, Gingeras TR, Lockhart DJ. High density synthetic oligonucleotide arrays. Nat Genet. 1999; 21:20–24. [PubMed: 9915496]

Lobe CG, Koop KE, Kreppner W, Lomeli H, Gertsenstein M, Nagy A. Z/AP, a double reporter for cre-mediated recombination. Dev. Biol. 1999; 208:281–292. [PubMed: 10191045]

Lossinsky AS, Wisniewski HM. Immunoultrastructural expression of ICAM-1 and PECAM-1 occurs prior to structural maturity of the murine blood-brain barrier. Dev Neurosci. 1998; 20:518–524. [PubMed: 9858840]

Mabie PC, Mehler MF, Marmur R, Papavasiliou A, Song Q, Kessler JA. Bone morphogenetic proteins induce astroglial differentiation of oligodendroglial-astroglial progenitor cells. J. Neurosci. 1997; 17:4112–4120. [PubMed: 9151728]

Matsugami TR, Tanemura K, Mieda M, Nakatomi R, Yamada K, Kondo T, Ogawa M, Obata K, Watanabe M, Hashikawa T, Tanaka K. From the Cover: Indispensability of the glutamate

transporters GLAST and GLT1 to brain development. Proc Natl Acad Sci U S A. 2006; 103:12161–12166. [PubMed: 16880397]

McCarty JH, Monahan-Earley RA, Brown LF, Keller M, Gerhardt H, Rubin K, Shani M, Dvorak HF, Wolburg H, Bader BL, Dvorak AM, Hynes RO. Defective associations between blood vessels and brain parenchyma lead to cerebral hemorrhage in mice lacking alphav integrins. Mol Cell Biol. 2002; 22:7667–7677. [PubMed: 12370313]

Mekki-Dauriac S, Agius E, Kan P, Cochard P. Bone morphogenetic proteins negatively control oligodendrocyte precursor specification in the chick spinal cord. Development. 2002; 129:5117–5130. [PubMed: 12399304]

Mishina Y, Suzuki A, Ueno N, Behringer RR. Bmpr encodes a type I bone morphogenetic protein receptor that is essential for gastration during mouse embryogenesis. Genes Dev. 1995; 9:3027–3037. [PubMed: 8543149]

Mishina Y, Hanks MC, Miura S, Tallquist MD, Behringer RR. Generation of Bmpr/Alk3 conditional knockout mice. Genesis. 2002; 32:69–72. [PubMed: 11857780]

Mishina Y. Function of bone morphogenetic protein signaling during mouse development. Front Biosci. 2003; 8:d855–d869. [PubMed: 12700086]

Muir EM, Adcock KH, Morgenstern DA, Clayton R, von Stillfried N, Rhodes K, Ellis C, Fawcett JW, Rogers JH. Matrix metalloproteases and their inhibitors are produced by overlapping populations of activated astrocytes. Brain Res Mol Brain Res. 2002; 100:103–117. [PubMed: 12008026]

Nakashima K, Yanagisawa M, Arakawa H, Kimura N, Hisatsune T, Kawabata M, Miyazono K, Taga T. Synergistic signaling in fetal brain by STAT3-Smad1 complex bridged by p300. Science. 1999a; 284:479–482. [PubMed: 10205054]

Nakashima K, Yanagisawa M, Arakawa H, Taga T. Astrocyte differentiation mediated by LIF in cooperation with BMP2. FEBS Lett. 1999b; 457:43–46. [PubMed: 10486560]

Ng CP, Hinz B, Swartz MA, M A. Interstitial fluid flow induces myofibroblast differentiation and collagen alignment in vitro. J Cell Sci. 2005; 118:4731–4739. [PubMed: 16188933]

Okano H. Stem cell biology of the central nervous system. J Neurosci Res. 2002; 69:698–707. [PubMed: 12205662]

Oohira A, Matsui F, Katoh-Semba R. Inhibitory effects of brain chondroitin sulfate proteoglycans on neurite outgrowth from PC12D cells. J Neurosci. 1991; 11:822–827. [PubMed: 2002362]

Parnavelas JG, Nadarajah B. Radial glial cells. are they really glia? Neuron. 2001; 31:881–884. [PubMed: 11580889]

Petersen W, Pufe T, Starke C, Fuchs T, Kopf S, Raschke M, Becker R, Tillmann B. Locally applied angiogenic factors--a new therapeutic tool for meniscal repair. Ann Anat. 2005; 187:509–519. [PubMed: 16320830]

Pierce EA, Foley ED, Smith LE. Regulation of vascular endothelial growth factor by oxygen in a model of retinopathy of prematurity. Arch. Ophthalmol. 1996; 114:1219–1228. [PubMed: 8859081]

Provis JM, Leech J, Diaz CM, Penfold PL, Stone J, Keshet E. Development of the human retinal vasculature: cellular relations and VEGF expression. Exp. Eye Res. 1997; 65:555–568. [PubMed: 9464188]

Rao MS. Multipotent and restricted precursors in the central nervous system. Anat Rec. 1999; 257:137–148. [PubMed: 10467245]

Raza SL, Cornelius LA. Matrix metalloproteinases: pro- and anti-angiogenic activities. J Investig Dermatol Symp Proc. 2000; 5:47–54.

Reiriz J, Espejo M, Ventura F, Ambrosio S, Alberch J. Bone morphogenetic protein-2 promotes dissociated effects on the number and differentiation of cultured ventral mesencephalic dopaminergic neurons. J. Neurobiol. 1999; 38:161–170. [PubMed: 10022564]

Rivieccio MA, John GR, Song X, Suh HS, Zhao Y, Lee SC, Brosnan CF. The cytokine IL-1beta activates IFN response factor 3 in human fetal astrocytes in culture. J Immunol. 2005; 174:3719–3726. [PubMed: 15749911]

Sakai K, Miyazaki J. A transgenic mouse line that retains Cre recombinase activity in mature oocytes irrespective of the cre transgene transmission. Biochem. Biophys. Res. Commun. 1997; 237:318–324. [PubMed: 9268708]

Samanta J, Burke GM, McGuire T, Pisarek AJ, Mukhopadhyay A, Mishina Y, Kessler JA. BMPR1a signaling determines numbers of oligodendrocytes and calbindin-expressing interneurons in the cortex. J Neurosci. 2003; 27:7397–7407.

Sango K, Oohira A, Ajiki K, Tokashiki A, Horie M, Kawano H. Phosphacan and neurocan are repulsive substrata for adhesion and neurite extension of adult rat dorsal root ganglion neurons in vitro. Exp Neurol. 2003; 182:1–11. [PubMed: 12821372]

Sapp E, Kegel KB, Aronin N, Hashikawa T, Uchiyama Y, Tohyama K, Bhide PG, Vonsattel JP, DiFiglia M. Early and progressive accumulation of reactive microglia in the Huntington disease brain. J Neuropathol Exp Neurol. 2001; 60:161–172. [PubMed: 11273004]

Saria A, Lundberg JM. Evans blue fluorescence: quantitative and morphological evaluation of vascular permeability in animal tissues. J Neurosci Methods. 1983; 8:41–49. [PubMed: 6876872]

See J, Mamontov P, Ahn K, Wine-Lee L, Crenshaw EB 3rd, Grinspan JB. BMP signaling mutant mice exhibit glial cell maturation defects. Mol Cell Neurosci. 2007; 35:171–182. [PubMed: 17391983]

Shin V, Zebboudj AF, Bostrom K. Endothelial cells modulate osteogenesis in calcifying vascular cells. J Vasc Res. 2004; 41:193–201. [PubMed: 15031603]

Sidky YA, Borden EC. Inhibition of angiogenesis by interferons: effects on tumor- and lymphocyte-induced vascular responses. Cancer Res. 1987; 47:5155–5161. [PubMed: 2441862]

Sorescu GP, Sykes M, Weiss D, Platt MO, Saha A, Hwang J, Boyd N, Boo YC, Vega JD, Taylor WR, Jo H. Bone morphogenic protein 4 produced in endothelial cells by oscillatory shear stress stimulates an inflammatory response. J Biol Chem. 2003; 278:31128–31135. [PubMed: 12766166]

Stone J, Itin A, Alon T, Pe'er J, Gnessin H, Chan-Ling T, Keshet E. Development of retinal vasculature is mediated by hypoxia-induced vascular endothelial growth factor (VEGF) expression by neuroglia. J. Neurosci. 1995; 15:4738–4747. [PubMed: 7623107]

Tagami M, Yamagata K, Fujino H, Kubota A, Nara Y, Yamori Y. Morphological differentiation of endothelial cells co-cultured with astrocytes on type-I or type-IV collagen. Cell Tissue Res. 1992; 268:225–232. [PubMed: 1617696]

Valdimarsdottir G, Goumans MJ, Rosendahl A, Brugman M, Itoh S, Lebrin F, Sideras P, ten Dijke P. Stimulation of Id1 expression by bone morphogenetic protein is sufficient and necessary for bone morphogenetic protein-induced activation of endothelial cells. Circulation. 2002; 106:2263–2270. [PubMed: 12390958]

West H, Richardson WD, Fruttiger M. Stabilization of the retinal vascular network by reciprocal feedback between blood vessels and astrocytes. Development. 2005; 132:1855–1862. [PubMed: 15790963]

Wine-Lee L, Ahn KJ, Richardson RD, Mishina Y, Lyons KM, Crenshaw EB 3rd. Signaling through BMP type 1 receptors is required for development of interneuron cell types in the dorsal spinal cord. Development. 2004; 131:5393–5403. [PubMed: 15469980]

Yamada M, Ivanova A, Yamaguchi Y, Lees MB, Ikenaka K. Proteolipid protein gene product can be secreted and exhibit biological activity during early development. J Neurosci. 1999; 19:2143–2151. [PubMed: 10066267]

Yuhki M, Yamada M, Kawano M, Iwasato T, Itohara S, Yoshida H, Ogawa M, Mishina Y. BMPRIA signaling is necessary for hair follicle cycling and hair shaft differentiation in mice. Development. 2004; 131:1825–1833. [PubMed: 15084466]

Zhang D, Mehler MF, Song Q, Kessler JA. Development of bone morphogenetic protein receptors in the nervous system and possible roles in regulating trkC expression. J Neurosci. 1998; 18:3314–3326. [PubMed: 9547239]

Zeinstra E, Wilczak N, Chesik D, Glazenburg L, Kroese FG, De Keyser J. Simvastatin inhibits interferon-gamma-induced MHC class II up-regulation in cultured astrocytes. J Neuroinflammation. 2006; 3:16. [PubMed: 16859542]

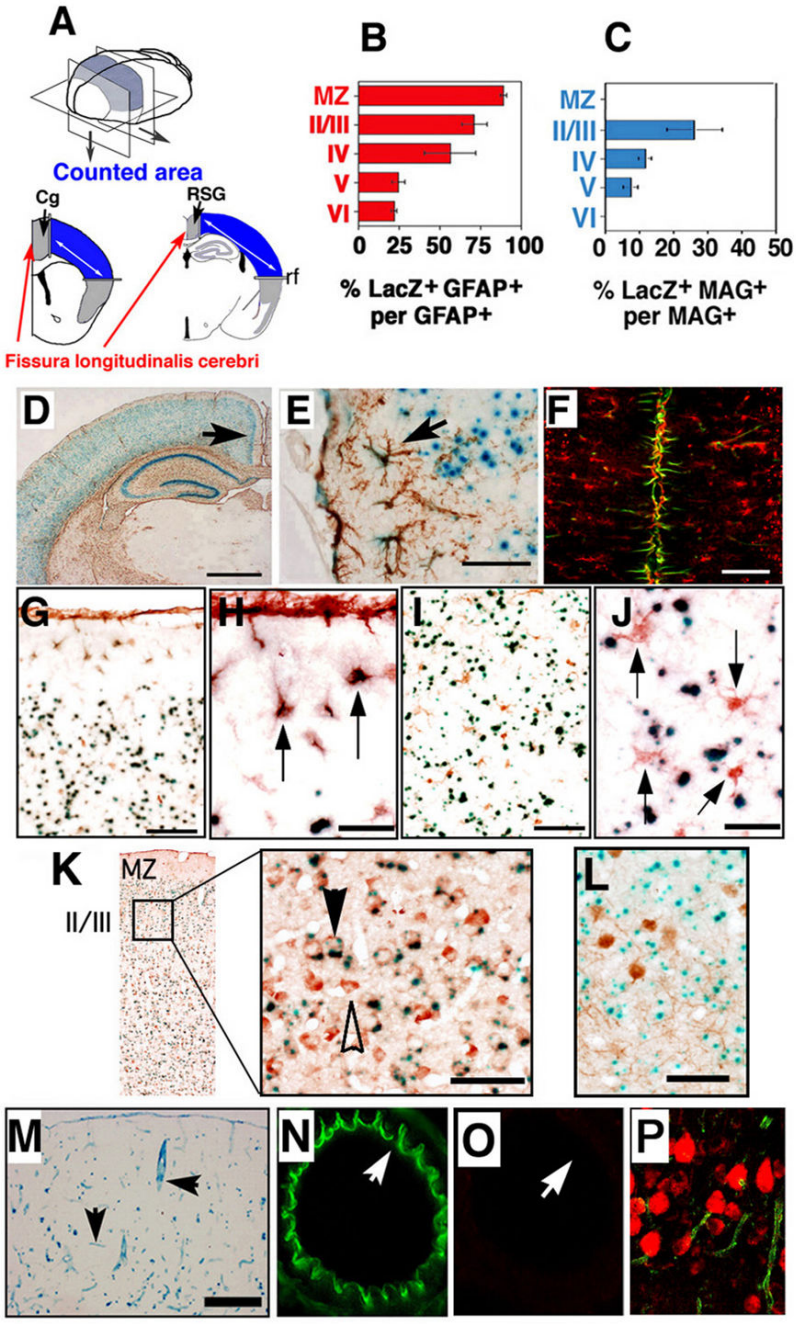

Figure 1. Specificity of Cre-mediated recombination in *Emx1-Cre* mice

(A) Experimental design: *Emx1*$^{Cre/+}$ mice were crossed to *CAG-CAT-LacZ* reporter mice to obtain double heterozygous (*Emx1-Cre/LacZ*) mice. At postnatal day 14 (P14), brains of double heterozygous *Emx1-Cre/LacZ* mice were sectioned and stained with X-gal, anti-GFAP antibody for astrocytes and anti myelin-associated glycoprotein (MAG) antibody for oligodendrocytes (brown DAB reaction product). GFAP-positive MAG-positive cells were counted in coronal sections of forebrain at Bregma from 1.0 mm to 2.5 mm (analyzed from anterior to posterior hippocampus with four consecutive sections analyzed per Bregma)

(Blue color area in panel **A**). Cg, cingulated cortex; RSG, retrosplenial granular; rf, rhinal fissure. (**B**) Ratio of double-positive LacZ GFAP cells to lacZ-positive cells in the designated area (see panel **A**) in left panel. Data are mean ± s.e.m. of $n = 4$ sections per animal, 3 animals; MZ indicates marginal zone. The number II–VI indicates cortical layers. (C) Ratios of double-positive cells for LacZ and MAG against total lacZ-positive cells were examined in the counted area (see panel **A**) in right panel. Data are given as mean ± s.e.m. of $n = 4$ sections per animal, 3 animals; MZ indicates marginal zone. The number II–VI indicates cortical layers. (**D**) Telencephalic GFAP-positive cells were detected in P14 *Emx1-Cre/LacZ* mice. Scale bar: 500 μm. GFAP-positive cells are brown. Arrow indicates fissura longitudinalis cerebri. (**E**) High magnification of (D). Double-positive cells (arrow) (β-Gal, blue; GFAP, brown) were detected in dorsal side of marginal zone around rf. Scale Bars; 50 μm. (**F**) The majority of astrocytes along the fissura longitudinalis cerebri expressed β-Gal activity. P14 *Emx1-Cre/LacZ* mice sections were stained with anti β-gal antibody (red) and anti-GFAP antibody (green). Scale bar: 100 μm. **(G, H)** Double-positive cells (arrow) (β-Gal activity, blue; S100-β, brown) were detected in the dorsal side of the MZ around rf. Scale Bars; 50 μm **(G)**, 200 μm **(H)**. **(I, J)** β-Gal activity (blue) did not co-localize with S100-β expression (brown, arrow) in the ventral side of the cortex in layer IV. Scale Bars; 50 μm **(I)**, 200 μm **(J)**. **(K) (C)** The double positive cells for LacZ and neural marker-Hu (brown) were detected in P14 *Emx1-Cre/LacZ* mice (left panel). High magnification of the left panel. Double-positive cells (black arrow) (β-Gal, blue; Hu, brown) were detected in cortical layer II / III. Several Hu positive cells were negative for β-Gal activity (white arrow). Scale Bars; 50 μm. (L) Telencephalic parvalbumin-positive cells (brown) detected in P14 *Emx1-Cre/LacZ* did not express lacZ (β-Gal activity, blue). Scale bar: 50 μm. **(M)** Double heterozygous *Emx1-Cre CMV-ZA/AP* mice displayed strong β-Gal activity in endothelial cells in cerebral blood vessels at P14 (arrows). Scale bar: 500 μm. However, AP activity was detected in the dorsal telencephalon (data not shown). **(N, O)** *E*xpression of Cre was examined in ECs in *Emx1-Cre/LacZ*. Expression of eNOS (Green) at P14, was examined in ECs in a middle cerebral artery of double heterozygous mice **(N)**. The same section was stained with β-Gal antibody (Red) to detect Cre activity **(O)**. No β-Gal activity was detected. White arrows indicate the same point of the section. **(P)** Panel (P) showed β-Gal antibody (Red) detected in cortical layers II and III of *Emx1-Cre/LacZ* mice at P14.

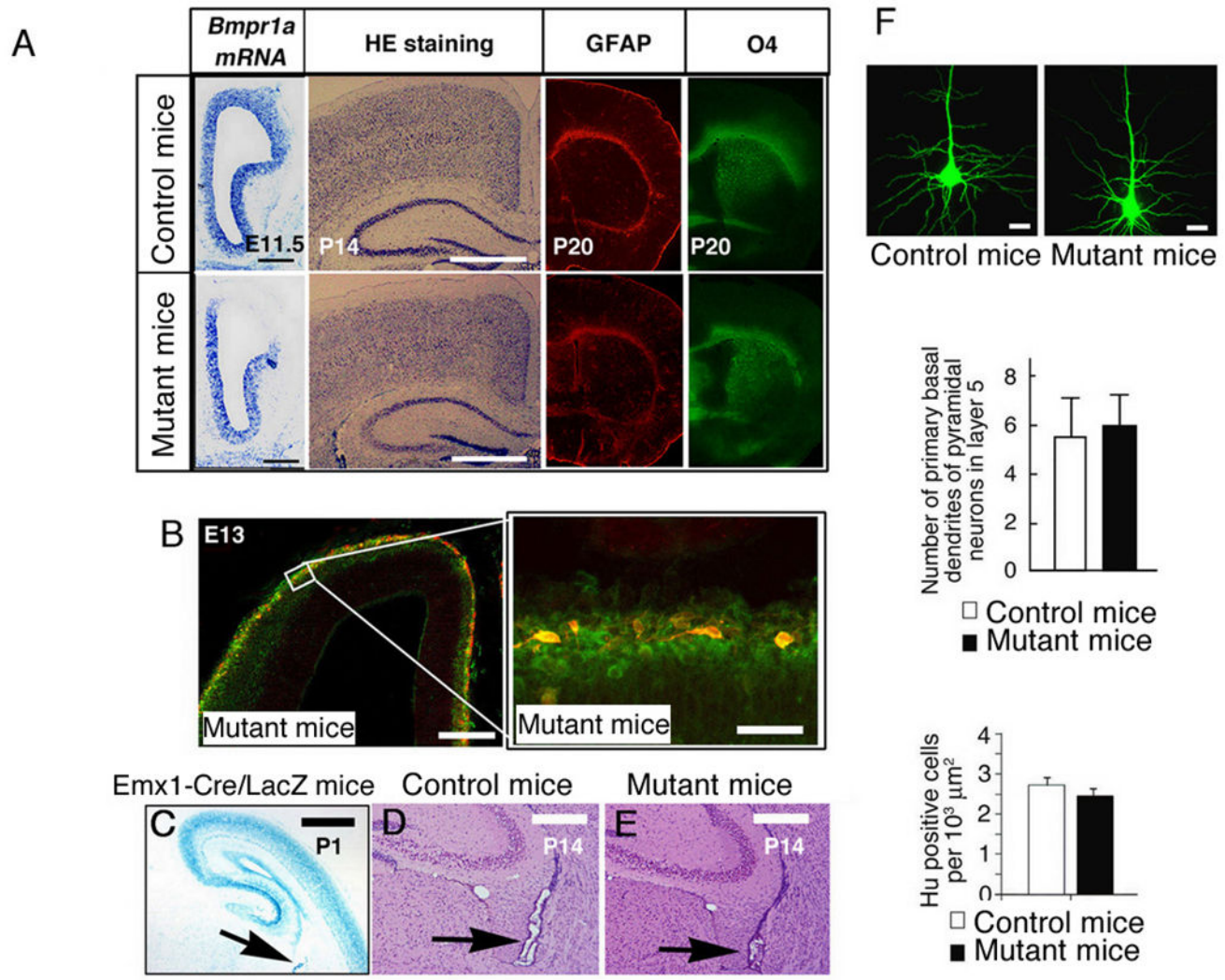

Figure 2. Cortical layer structure in the telencephalic region of the mutant mice

(A) *Bmpr1a* mRNA expression pattern in the left side of transverse section from telencephalon in E11.5 *Emx1*$^{+/+}$ *Bmpr1a*$^{+/-}$ mice (control mice; upper panel) and *Emx1*$^{Cre/+}$ *Bmpr1a*$^{flox/-}$ mice (mutant mice; lower panel). Scale bar: 200 μm. . Sections from the control (upper panel) and mutant mice (lower panel) at P14 were stained with Hematoxylin (HE). No overt changes in cortical neural layers were observed. Scale bar: 500 μm. GFAP staining in the telencephalon of P0 the control (upper panel) and mutant mice at P20 (lower panel). O4, oligodendrocyte marker, staining in the telencephalon of the control (upper panel) and mutant mice (lower panel). **(B)** Migration of Cajal-Retzius cells and hippocampal structure in the mutant mice. Tangential migration of Cajal-Retzius cells was presenting in primordial plexiform zonal at E13 cortex in brains of the mutant mice. Cajal-Retzius cells visualized with anti-calretinin (red) migrated tangentially to populate the cortical surface, derived from the cortical hem. Neurons in the primordial plexiform zone were stained with MAP2 antibody (Green). (right) Higher magnification of (left). **(C)** Brains from *Emx1-Cre/LacZ* mice were sectioned and stained with X-gal at P1. Cre activity was evident in the

choroid plexus (arrow). **(D, E)** HE staining of histological sections of brains including choroid plexus at P14. The choroid plexus of the mutant mice (E) was appeared. Scale Bars; 500 μm (C), 200 μm (A, D, E), 50 μm (B). **(F)** Morphology of pyramidal neurons and number of cortical neurons in layer V. Pyramidal neurons in layer V were visualized by injecting Lucifer yellow into cortical slices from P14 brains. Scale bar: 20 μm. Primary basal dendrites of pyramidal neurons in layer V; the average of three experiments is shown; twenty pyramidal cells were examined per experiment. Density of Hu (number of neural nuclei per 1000 μm^2) was measured at P0 on neural layers in layers II to VI at Bregma from 1.0 mm to 2.5 mm. Sections were analyzed from anterior to posterior with four consecutive sections per Bregma). There was no significant difference in the number of neurons between the control and mutant mice (Data are mean ± s.e.m., $n = 4$ sections per animal, 3 animals, P = 0.285).

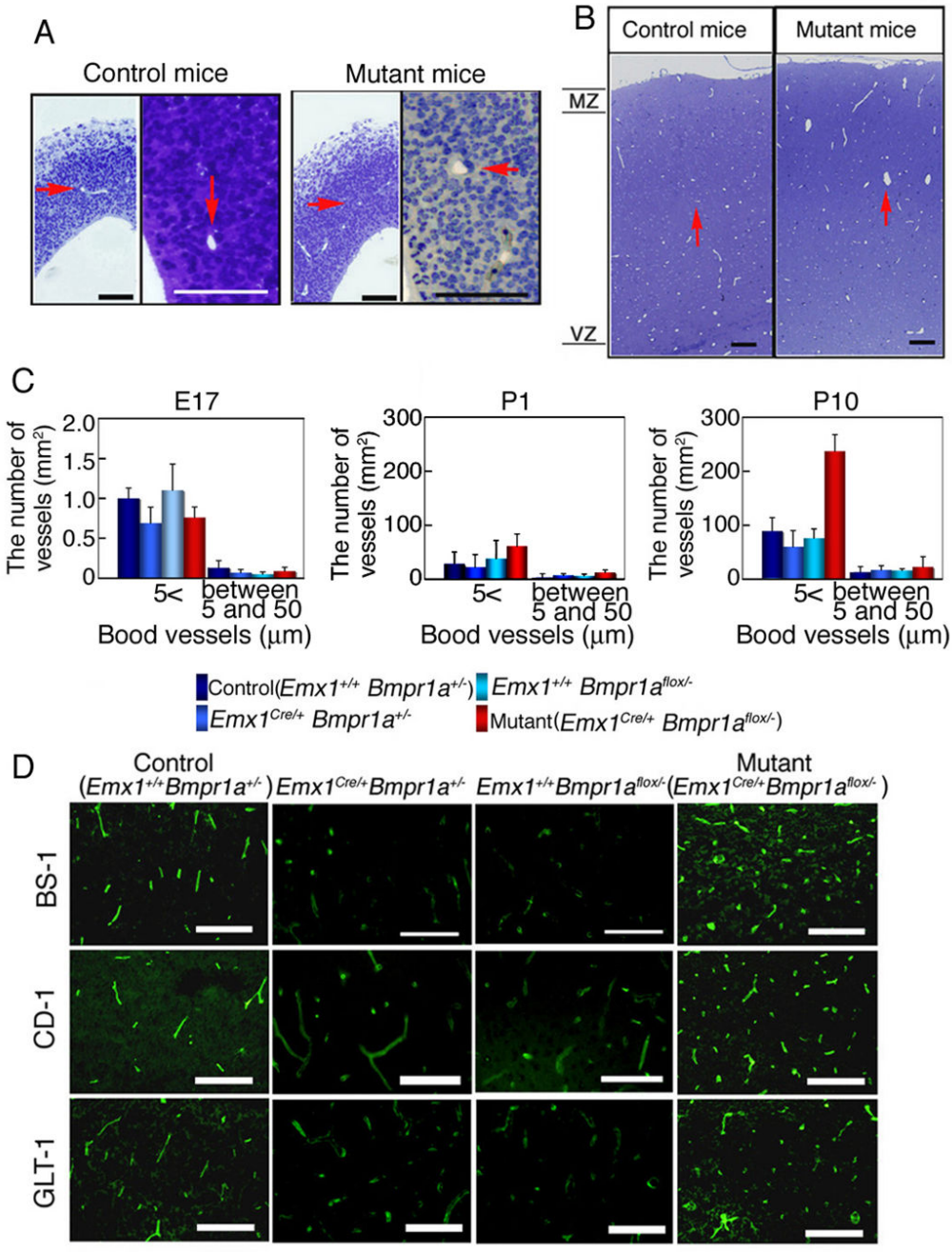

Figure 3. Glial BMPRIA signaling is essential for the termination of angiogenesis

(A) Semi-thin sections (1 μm, thickness) from cortex at E17 were stained with toluidine blue (A). Red arrows indicate cerebral blood vessels. Scale bar: 50 μm. . **(B)** Semi-thin sections (1 μm, thickness) from cortex at P10 were stained with toluidine blue. Red arrows indicate cerebral blood vessels. Scale bar: 100 μm. **(C)** The numbers of blood vessels counted at E17 (A), P1 (not shown) and P10 (B) were classified in two groups based on their diameter. Results in all 4 genotypes were shown. The number of cerebral blood vessels was similar in the control and mutant mice at E17 and P1, however, the mutant mice had more cerebral

blood vessels than control mice at P10 (blood vessels between 5 and 50 μm in diameter). **(D)** P10 Cortical layers of II and III in the mutant mice (*Emx1*$^{Cre/+}$ *Bmpr1a*$^{flox/-}$) mice had more small blood vessels than *Emx1*$^{+/+}$ *Bmpr1a*$^{+/-}$ (as the control), *Emx1*$^{Cre/+}$ *Bmpr1a*$^{+/-}$, and *Emx1*$^{+/+}$ *Bmpr1a*$^{flox/-}$ mice, as detected by Lectin BS-1, PECAM-1/CD31, and GLT1 immunoreactivity. Scale bars 100 μm.

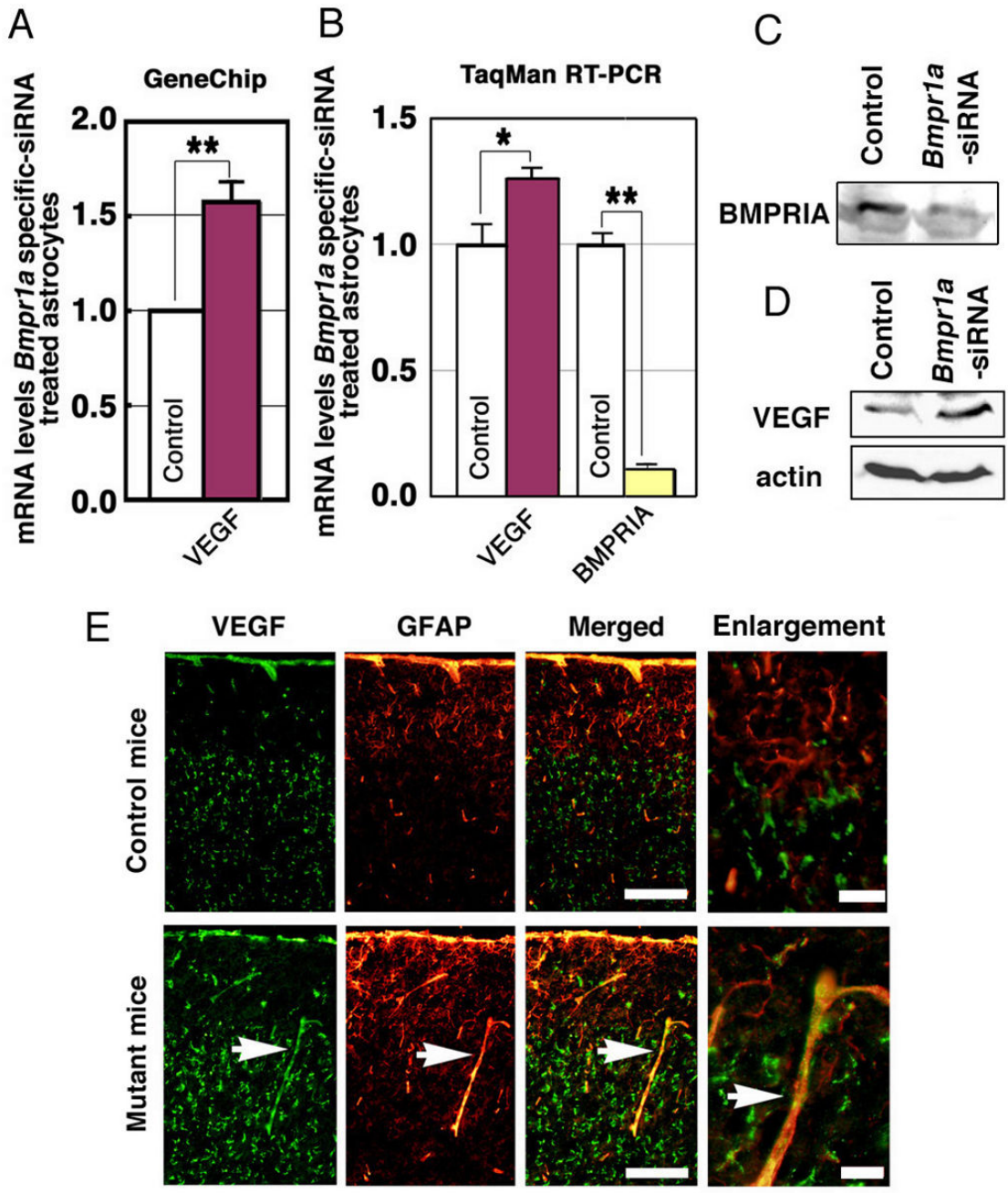

Figure 4. *Bmpr1a* silencing affects VEGF expression *in vitro*

(A) VEGF is downregulated by treatment with *Bmpr1a*–targeted siRNA. GeneChip analysis (Murine genome U74Av2) was performed on astrocytes treated with *Bmpr1a*-targeted or nonspecific siRNA. Data are expressed as relative expression of the VEGF in astrocytes treated with specific or nonspecific siRNA (mean ± s.e.m.). $^{**}P < 0.001$ (Student *t*-test). **(B)** VEGF was upregulated by *Bmpr1a*-targeted siRNA. TaqMan RT-PCR analysis (Applied Biosystems) was performed using samples from astrocytes treated with specific or nonspecific siRNA (See method section). Data are expressed as relative expression of

procollagen in astrocytes treated with specific and nonspecific siRNA (n = 4 for each group; mean ± s.e.m.; *$P < 0.05$, **$P < 0.001$ (Student *t*-test). **(C)** Western blot of astrocytes treated with specific or nonspecific siRNA, using an anti-BMPRIA antibody. **(D)** Western blot of astrocytes treated with specific or nonspecific siRNA, using an anti-VEGF polyclonal antibody. **(E)** Co-expression of VEGF and GFAP in cortical astrocytes around cortical blood vessels at P10. Astrocytic VEGF immunoreactivity, which is normally downregulated at P10, was significantly upregulated in the mutant mice (white arrows). Scale bars (white) are 100 μm. Right panels show higher magnification of left merged panel. Scale bars (red) are 20 μm.

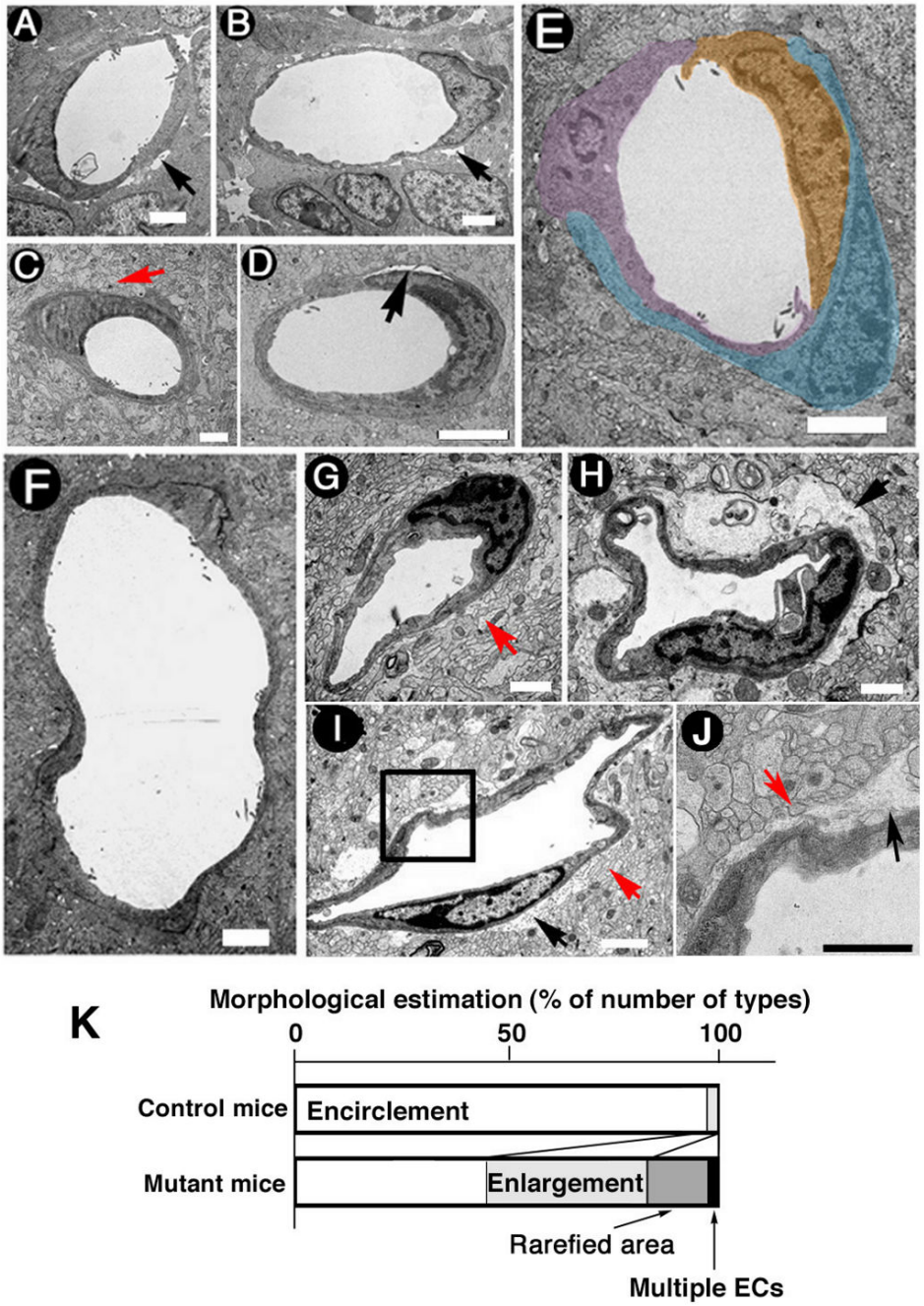

Figure 5. Loss of BMPRIA signaling leads to cerebral vascular malformation *in vivo*

(A, B) Electron microscope (EM) images of intercortical blood vessel crossections indicated that cerebral ECs were not attached to surrounding cells and the BBB was unformed in both the control (A) and the mutant mice (B) at E17. Scale Bars: 1 μm. **(C)** A crossectional EM image of intercortical blood vessel crossections in the control mice at P10 showed that astrocytic endfeet were attached to ECs. Scale bar: 1 μm. **(D)** A crossectional EM image of intercortical blood vessels showed that cerebral ECs were not attached to surrounding cells and the BBB was defective in the mutant mice at P10. Scale Bar: 1 μm. **(E, F)** Vessels in the

mutant mice at P10 showed other two abnormal types of structures, vessels surrounded by multiple ECs (E) and enlarged vessels (F). Scale Bar: 1 μm. **(G)** A crossectional EM image of intercortical blood vessels in the control mice at P20 indicated that astrocytic endfeet were attached to ECs. **(H, I)** Malformation of BBB in the mutant mice at P20 was confirmed using EM. **(J)** High magnification of a boxed area in panel (I) indicates a gap of cells. Red arrow indicates astrocytic endfeet. Black arrow indicates defective attachment between ECs and astrocytes. Scale bar: 1 μm. **(K)** The ratio of classified structure of a blood vessel in four types (encirclement-type, rarefied area-type, enlargement-type, and multiple ECs-type) in the control and mutant mice at P10 were presented. One hundred sixty five and 240 of individual small blood vessels from the control and mutant mice, respectively, were observed and classified.

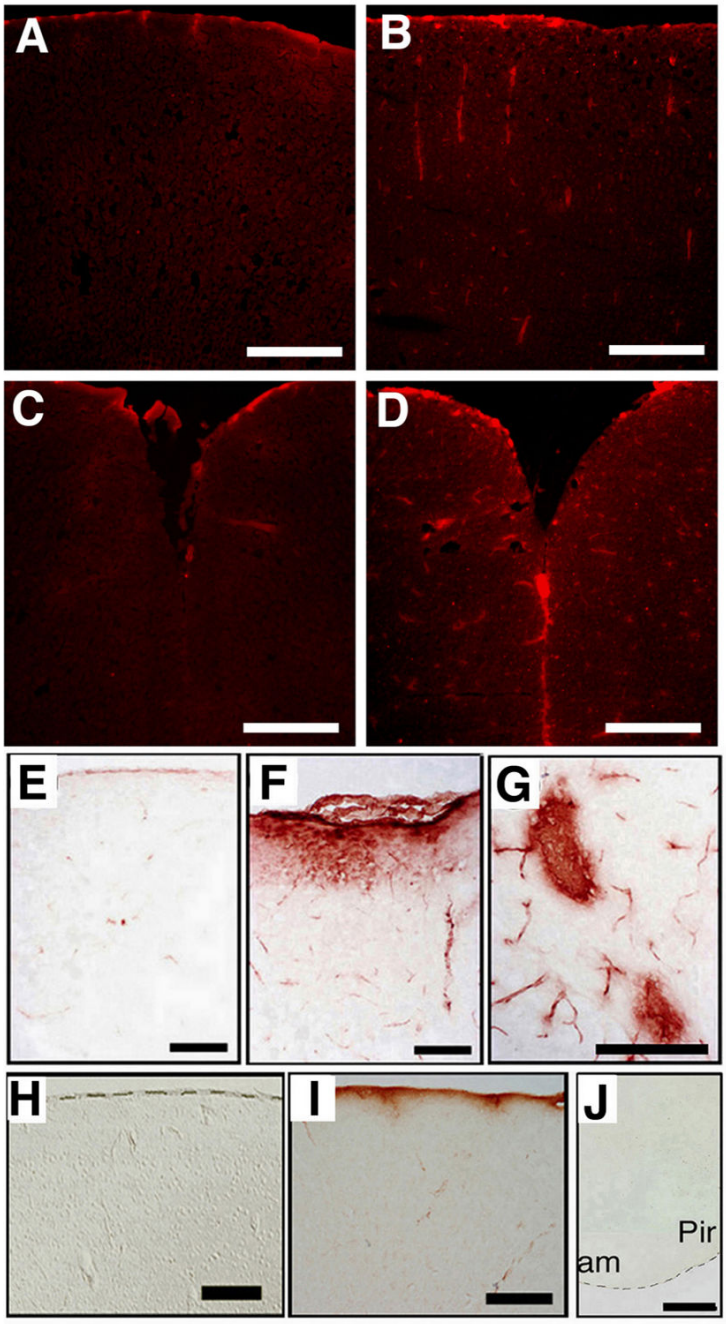

Figure 6. Loss of BMPRIA signaling leads to IgG leakage *in vivo*

(A–D) Leakage of cortical vascular vessels was visualized using Evans blue (EB) dye (excitation at 620 nm, emission at 680 nm). No leakage of EB was observed in cortical sections of the control mice at P10 (A). Leakage of EB was apparent in the dorsal parts of telencephalon of the mutant mice at P10 (B). No leakage of EB was observed in the cinglate and retrosplenial cortices (Cg/RS) along the fissura longitudinalis cerebri sections of the control mice at P10 (C). Leakage of EB was observed in the Cg/RS along the fissura longitudinalis cerebri. sections of mutant mice at P10 (D). **(E–J)** Leakage of cortical

vascular vessels was visualized by detection of immunoglobulin with anti-mouse IgG antibody. No leakage of IgG (DAB staining, Brown color) in cortical sections of the control mice at P20 (E). Leakage of IgG was detected in superficial cortex (F) and in Cg/RS (G) of the mutant mice at P20. No leakage of IgG was observed in superficial cortex of the control mice at 10 month (H). Leakage of IgG was detected in the same area of the mutant mice at 10 month (I). No IgG leakage was observed in amygdaloid sections of the mutant mice at 10 month (J). Scale bar: 200 μm (A–D), 400 μm (E–G), 500 μm (H–J). Pir, piriform cortex; am, amygdaloid.

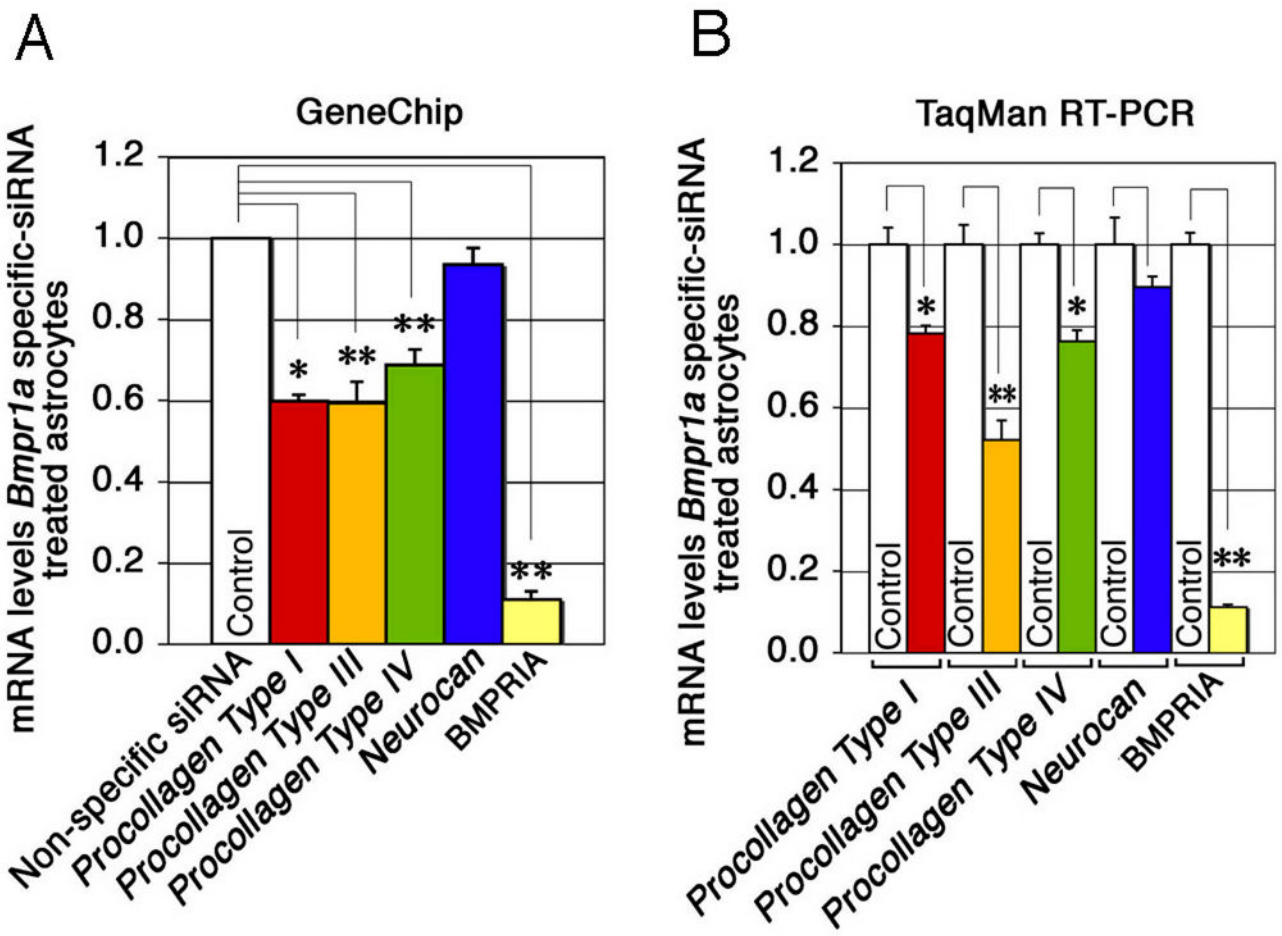

Figure 7. *Bmpr1a* silencing affects glial adhesion *in vitro*

(A) Collagens were downregulated by *Bmpr1a*–specific siRNA. GeneChip analysis (Murine genome Array U74Av2) was performed on astrocytes treated with *Bmpr1a*-specific or nonspecific siRNA. Data are expressed as relative expression of procollagen in astrocytes treated with specific or nonspecific siRNA (mean ± s.e.m.). $*P < 0.05$, $**P < 0.001$ (Student *t*-test). **(B)** Collagens were downregulated by *Bmpr1a*-specific siRNA. TaqMan RT-PCR analysis (Applied Biosystems) was performed using samples from astrocytes treated with specific or nonspecific siRNA (See method section). Data are expressed as relative expression of procollagen in astrocytes treated with specific and nonspecific siRNA (n = 4 for each group; mean ± s.e.m.; $*P < 0.05$, $**P < 0.001$ (Student *t*-test).

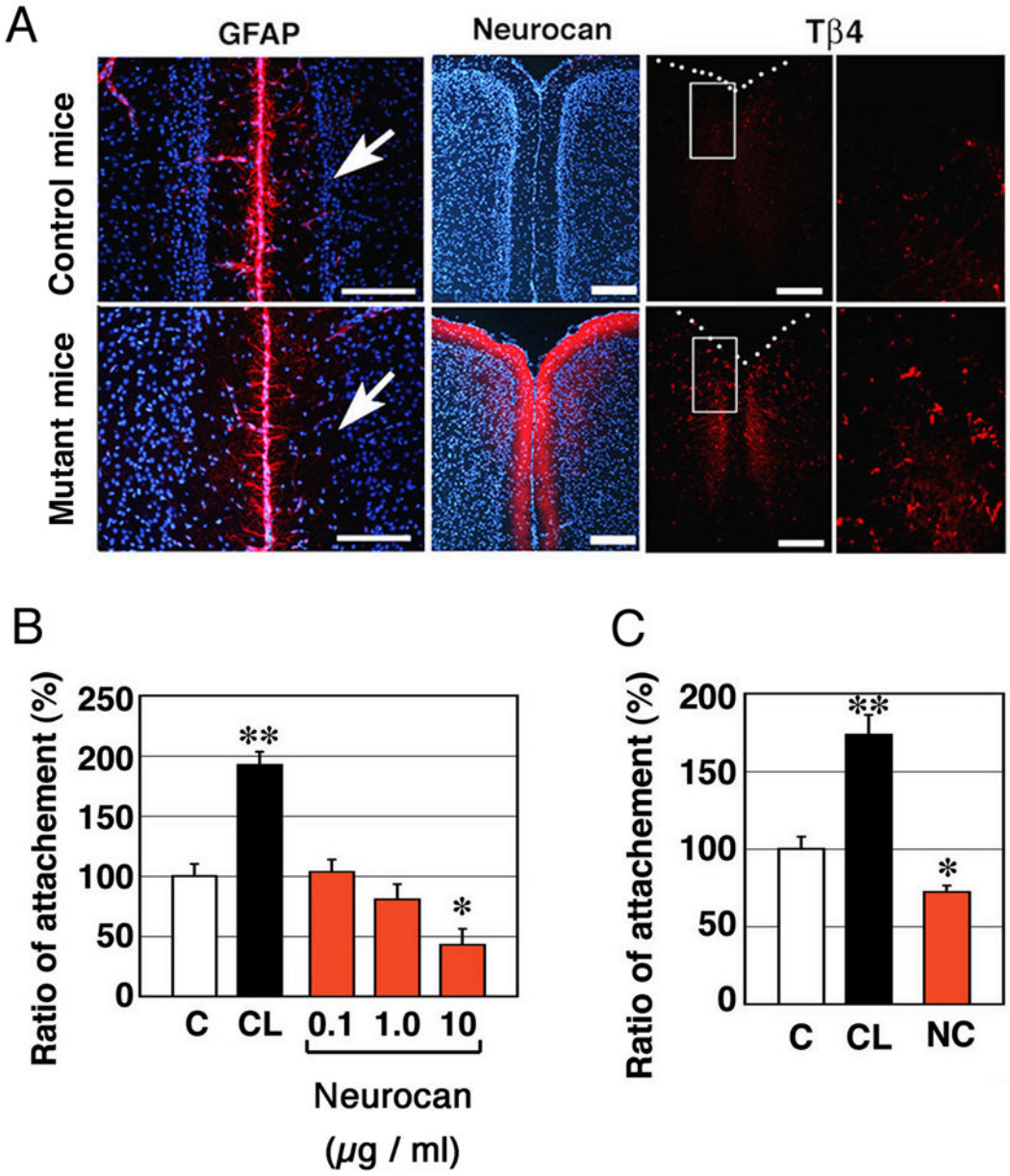

Figure 8. Loss of BMPRIA signaling leads inflammation response

(A) Fissura longitudinalis cerebri in the 10-month-old mutant mice were stained with anti-GFAP Ab, anti-neurocan (NC) Ab and anti-thymosin β4 (Tβ4), a microglial marker, in the 10-month-old control mice. Right panels show higher magnification of boxed areas in left panels. Nuclei were stained with Hoechst dye (blue). Scale Bars; 200 μm. (B) Endothelial cells were plated on a cell culture dish coated with 20 μg / ml collagen (CL) or 10 μg/ml neurocan. Attachment of TM-BBB cells as a function of neurocan dose. (C) Same as (B) using 10 μg/ml neurocan and human umbilical vein endothelial (HUVEC) cells. Data are mean ± s.e.m. ($n = 8$). Statistical significance was determined using Student's t-test (*, $P < 0.05$; **, $P < 0.001$).